EARTH OBSERVATION DATA ANALYSIS

Remote Sensing of Vegetation from MODIS

Ivan Colantoni

1704031

colantoni.1704031@studenti.uniroma1.it

Federico Parente

1716030

parente.1716030@studenti.uniroma1.it

Contents

1 Introduction **2**
1.1 Data Quality Check 2

2 Data Analysis **3**
2.1 Spectrum 3
2.2 Histograms 3
2.3 Profile Plot 4

3 Data Correlation **4**
3.1 ROI 5

4 Principal Component Analysis **5**

5 Classification **6**
5.1 Unsupervised 6
5.2 Supervised 6

6 Vegetation Index **7**
6.1 2-bands 7
6.2 3-bands 8
6.3 Classification NDVI 9
6.4 Summer-Winter comparison 9
6.5 Change Detection 10

References **10**

1 Introduction

Objective: explore MODIS satellite data and apply SNAP classification tools and vegetation indexes. For this Homework we have selected a MODIS product at a 1Km resolution over Italy. Details of the image are reported in the figure 1

Figure 1: Product Details

Geolocation_File	MYD03.A2019208.1155.061.2019209145601.hdf
Start_Time	2019-07-27 11:55:00.000000
End_Time	2019-07-27 12:00:00.000000
MODIS_Resolution	1km
MODIS_Platform	Aqua

1.1 Data Quality Check

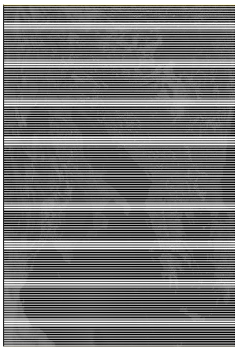

Figure 2: Stripes

At the first stage we performed a data quality check on all the channels available of the product. We found out that the EV_500_Aggr_1km_RefSB6 *(Earth View 500M Aggregated 1km Reflective Solar Bands Scaled Integers)* channel has failures/stripes and can't be used for data analysis. See figure 2. It is now possible to see the RGB picture of the product, setting:

```
Red−channel = EV_250_Aggr1km_RefSB_1 (645nm)
Green−channel = EV_500_Aggr1km_RefSB_4 (555nm)
Blue−channel = EV_500_Aggr1km_RefSB_3 (469nm)
```

and resulting in the image of figure 3

Figure 3: RGB Image Product

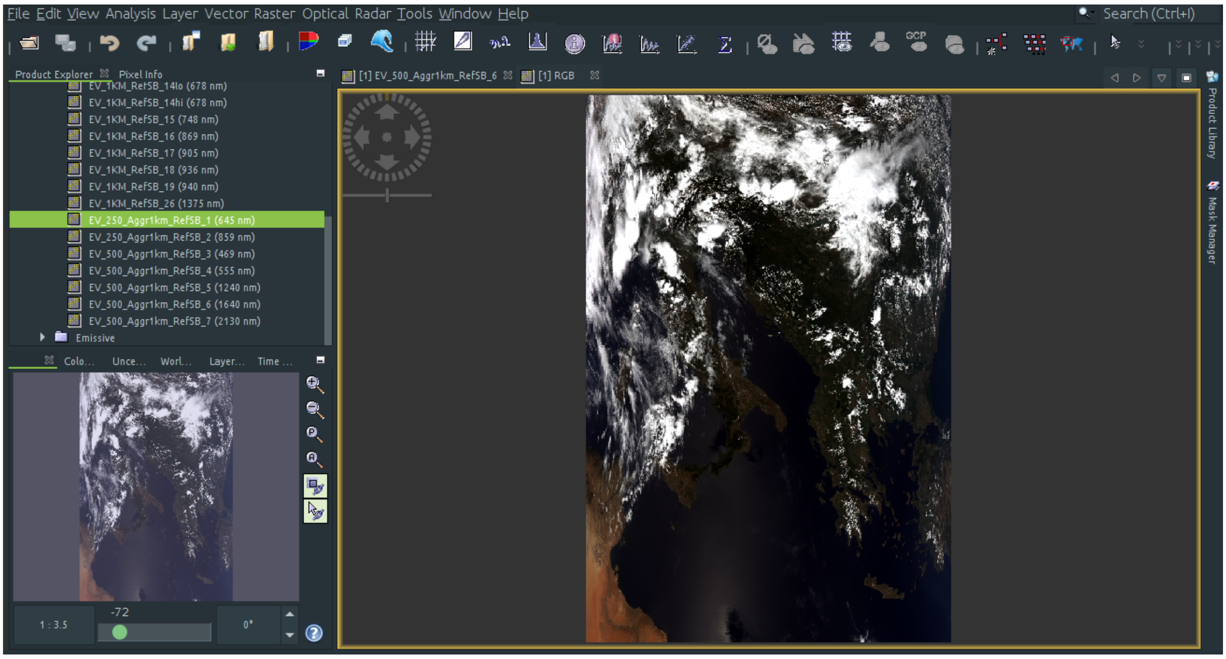

2 Data Analysis

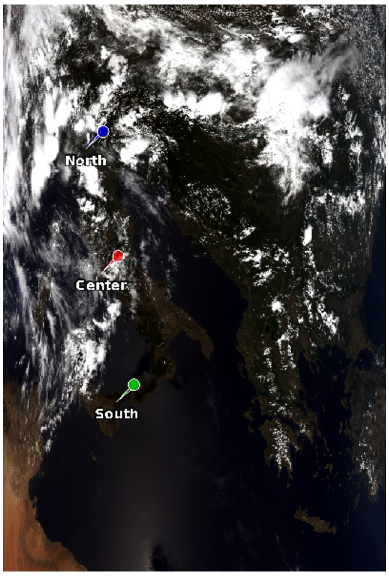

Figure 4: Pin positioning

In order to perform data analysis we added three pins to the image using the Pin-placing-tool in the toolbar window and placed them into interesting positions i.e: North, Center, South. See figure 4.

2.1 Spectrum

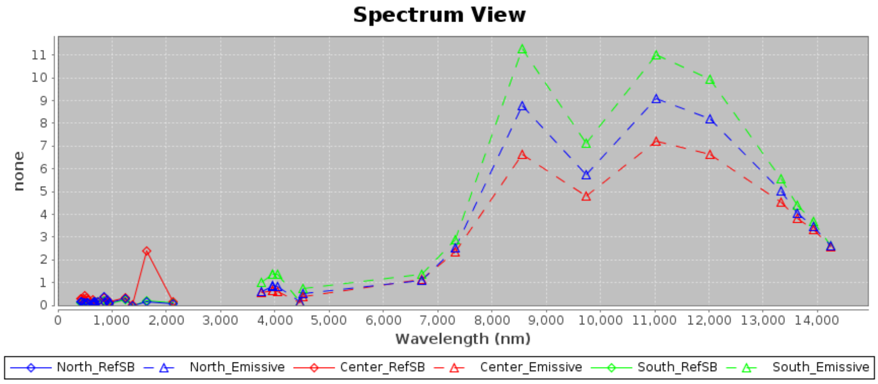

Figure 5: Spectrum View

From this points, we are able to compute the spectrum views associated to the spectral band values of each pin, and plotting them with *Optical/Spectrum View* tool. Results are showed here in figure 5

2.2 Histograms

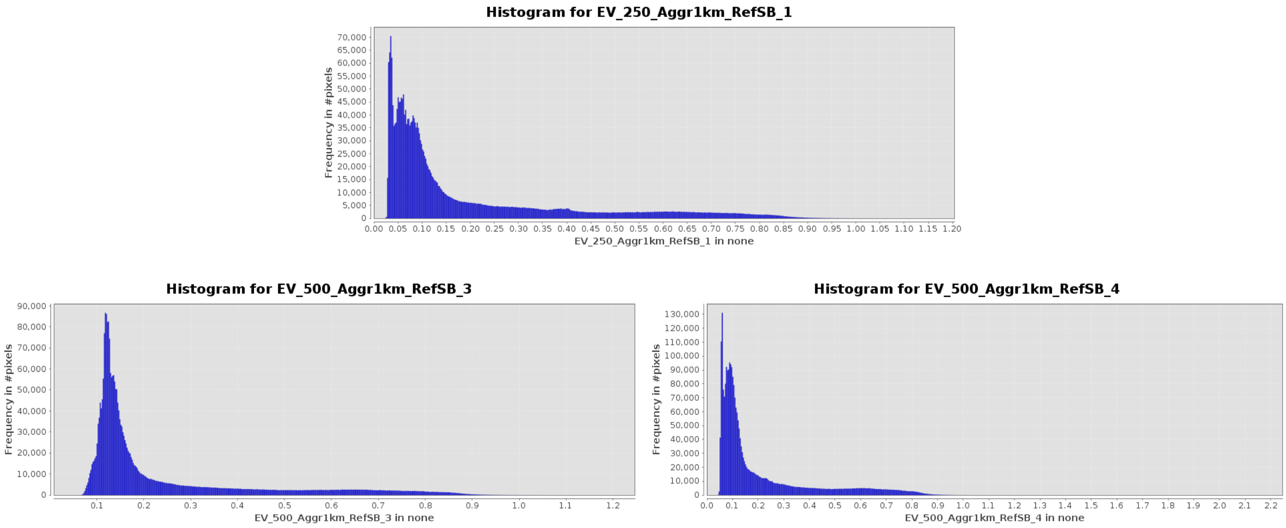

Figure 6: Histograms

We then plotted the histograms related to the bands used to build the RGB image (RefSB1, RefSB4, RefSB3), giving an idea of the frequency the values of each channel appears with respect to the pixels. Results showed in figures 6

2.3 Profile Plot

Introducing a geometry, a line crossing the three pins showed in figure 9, we performed a profile plot along that shape, which shows the value of the selected band constrained the bounds of the line. We provide the resulting plot for channel B1, showed in figure 7

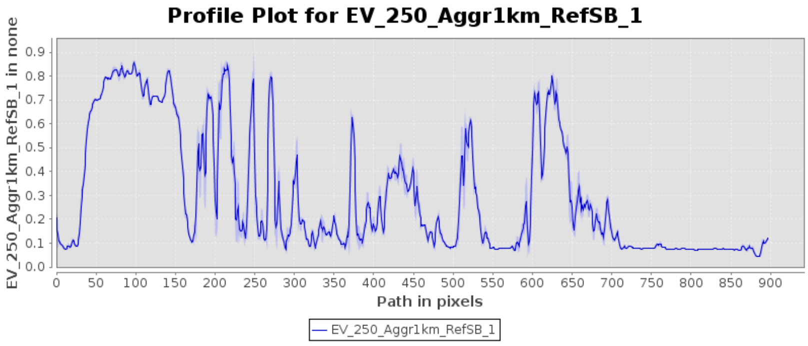

Figure 7: Profile Plot

3 Data Correlation

Using the *Analysis/Scatter Plot* tool, we analyzed the correlation of the RGB channel for the whole image. In figure 8, we provide such correlation in the following order plotting

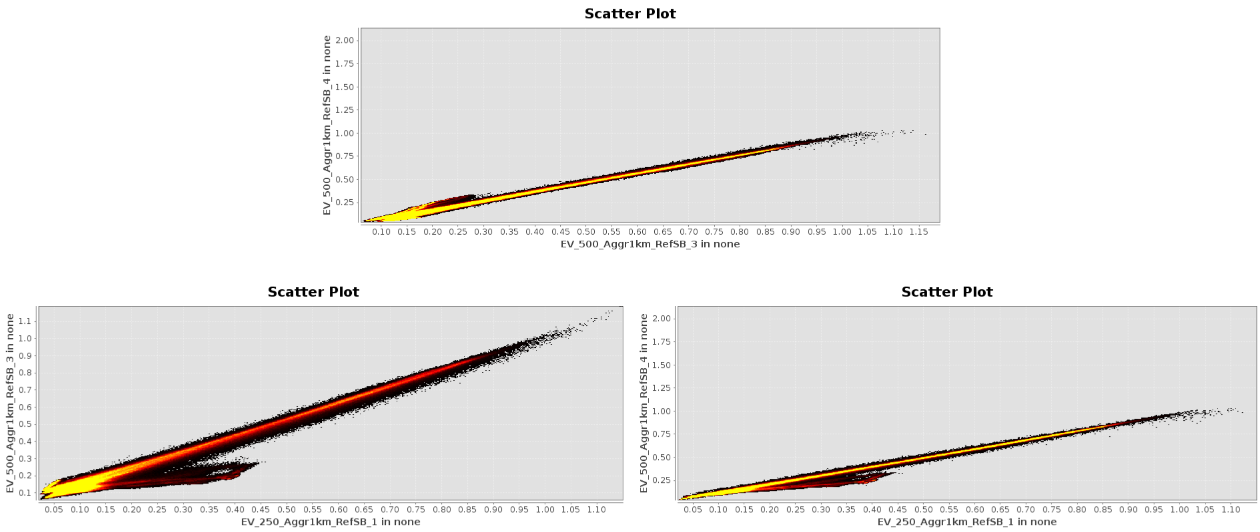

Figure 8: Correlation of RGB channels

3.1 ROI

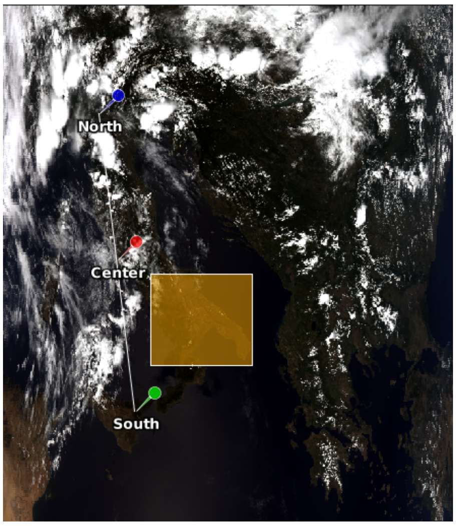

Figure 9: Geometries

Introducing a ROI (Region of Interest), showed in figure 9 the resulting correlation of the RGB channel is displayed in figure 10

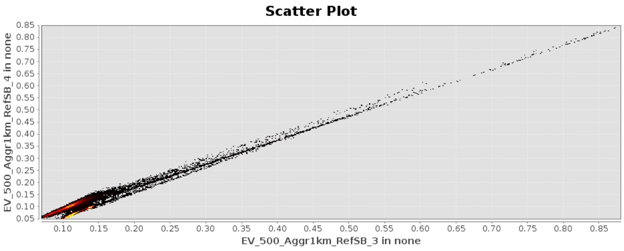

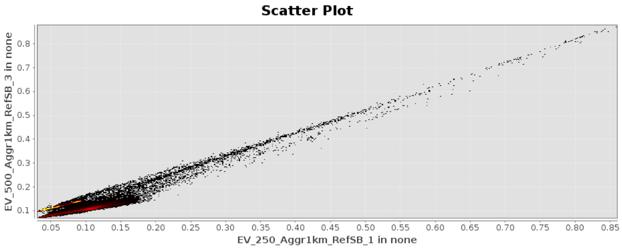

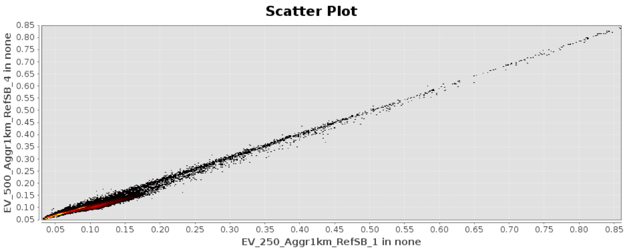

Figure 10: Correlation of RGB channels (ROI)

4 Principal Component Analysis

We performed PCA over the 6 reflective bands and report here the view of the first 2 components (fig. 11)

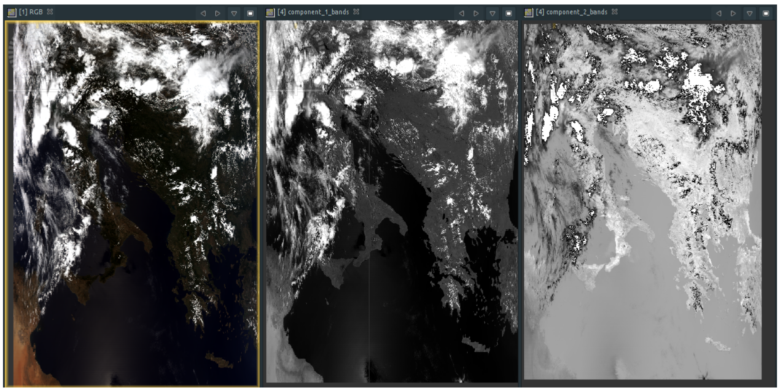

Figure 11: Principal Component Analysis

5 Classification

5.1 Unsupervised

Performing unsupervised classification using K-means algorithm, as defined in *Raster/Classification/Unsupervised Classification/k-means Clusters Analysis*. In the experiment we initially set 1 band channel (RefSB1), 3 classes (Sea, Land, Cloud) and 30 iterations of the algorithm (fig. 12 right side). Results were poor and we improved the number of bands to be processed up to 6. As showed in the left side of fig. 12 this led us to a reasonable result and even increasing the number of iterations we don't get much better.

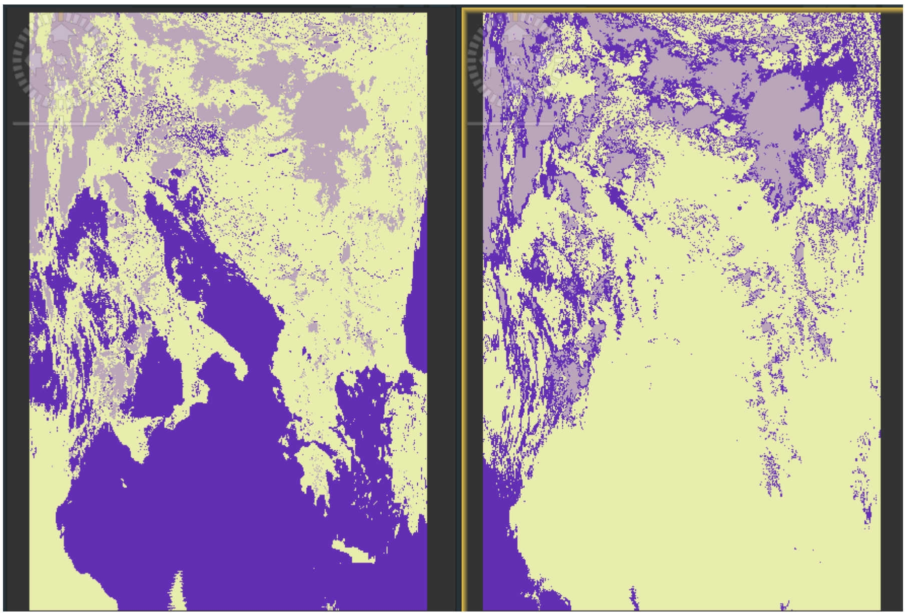

Figure 12: K-means clustering

5.2 Supervised

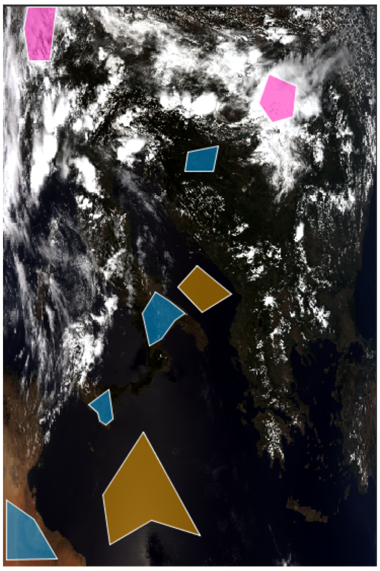

Figure 13: Geometries

To perform a supervised classification we first converted the *.hdf* product to *BEAM-DIMAP* format and stored locally the RGB bands into virtual ones to be used later. Then we create a data container with geometries, which holds the values of our bands bounded in the selected regions (see fig. 13). Then we ran *Raster/-Classification/Supervised Classification/Maximum Likelihood Classifier*. The results in fig.14 is showed on the right and compared with the unsupervised one.

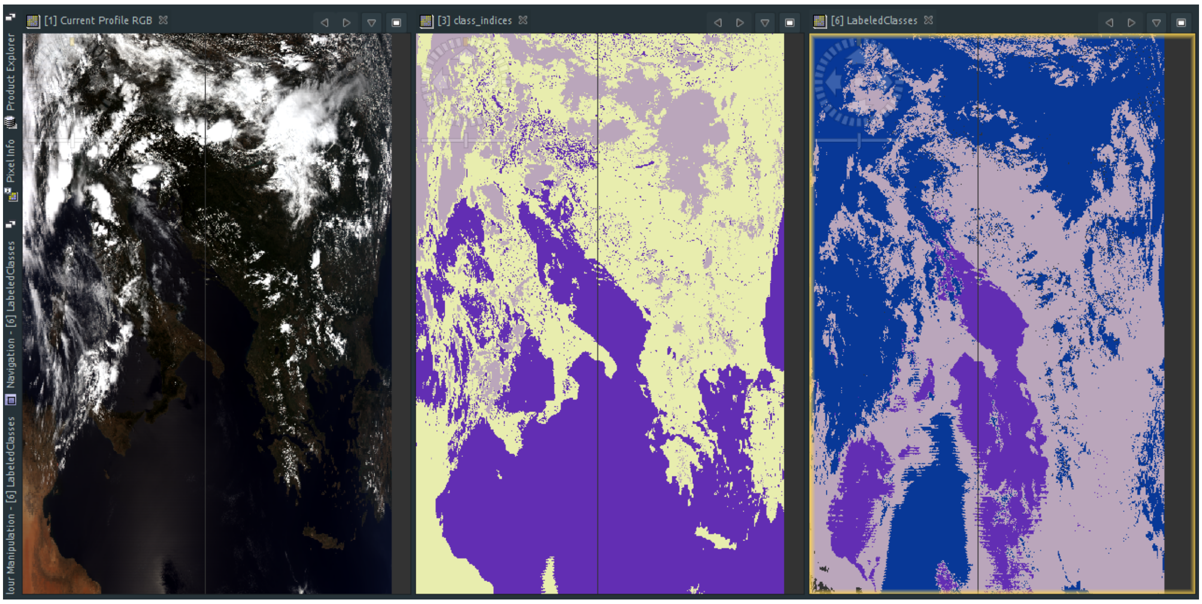

Figure 14: Classifications

6 Vegetation Index

6.1 2-bands

There exists various vegetation indexes (VI) exploiting 2 or 3 bands [2] [1]. For the class of 2-bands we implemented the canonical Normalized Difference Vegetation Index (NDVI).
$NDVI = \frac{NIR-RED}{NIR+RED} \in [-1, 1]$, and the simple ratio: $RVI = \frac{NIR}{RED} \in [0, +\inf]$
The rationale of that indexes belongs to a physical property of the plants, which are well known to absorb the solar radiation as a form of energy. Green leaves reflect the radiation in the NIR spectral region while absorbing the RED spectral region. On the other hand, clouds, snow and water reflect the radiation in the RED spectral region while absorbing the NIR one. As a consequence the higher is the value of NDVI (or RVI) the higher is the presence of green and health plants. Results are showed in fig. 16 and 15 - The RVI index is always positive but has infinite values, which can lead to disadvantages in practical applications (i.e the palette colouring).

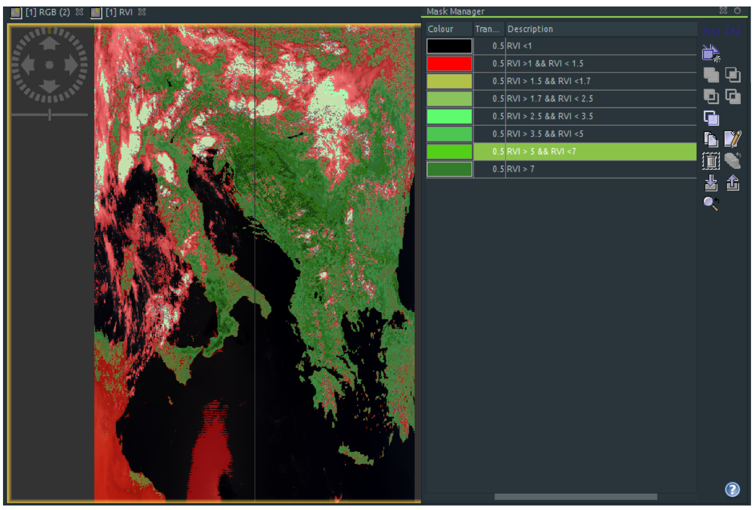

Figure 15: RVI

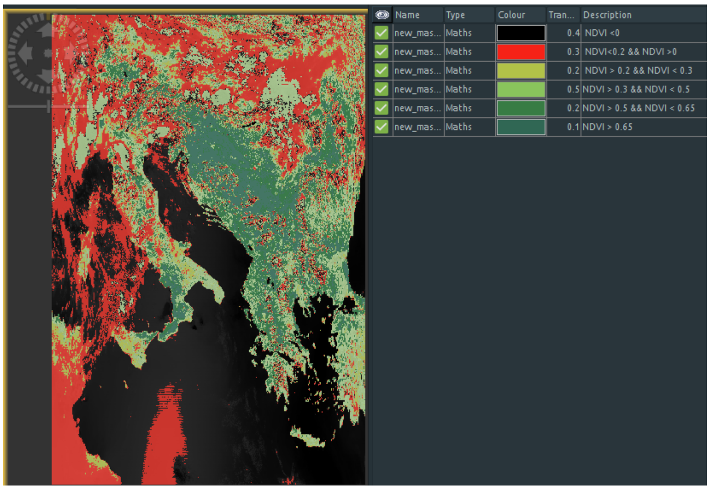

Figure 16: NDVI

6.2 3-bands

The EVI Enhanced Vegetation Index is an optimized VI designed to enhance the vegetation signal with improved sensitivity in high biomass regions and improved vegetation monitoring through a de-coupling of the canopy background signal and a reduction in atmosphere influences. With respect to NDVI there are some advantages:

- Correcting for some distortions in the reflected light caused by the particles in the air as well as the ground cover below the vegetation (Blue, L).
- Avoiding saturation as easily as the NDVI when viewing rainforest and other areas of the Earth with large amounts of chlorophyll (C1, G).

EVI is computed following this equation:
$EVI = G \times \frac{NIR - RED}{NIR + C1 \times RED - C2 \times BLUE + L}$,
in **MODIS-EVI** algorithm :
$L = 1(Canopyadjustement), C1 = 6(aerosolcoefficient1)$
$C2 = 7.5(aerosolcoefficient2), G = 2.5(Gainfactor)$

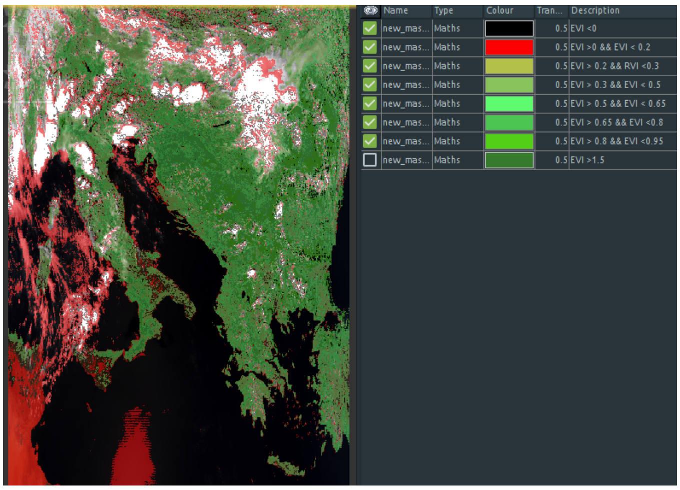

Figure 17: Enhanced Vegetation Index (EVI)

6.3 Classification NDVI

Applying k-means clustering algorithm with 3 classes to the NDVI index computed before, we got the result showed in fig.18. We think this is an admissible result, if compared to those obtained with MODIS channels, considering that only 2-bands were used to compute the index.

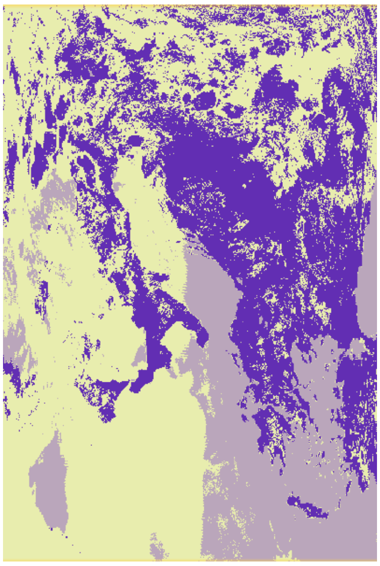

Figure 18: K-means clustering on NDVI index

6.4 Summer-Winter comparison

We selected an image taken on *2019-02-19* during winter season and applied the same NDVI index and the same mask used in summer period. In figure 19 it is visible the presence of snow on the mountains marked as black, which is not the case for the summer, and the green zone of the coastal areas.

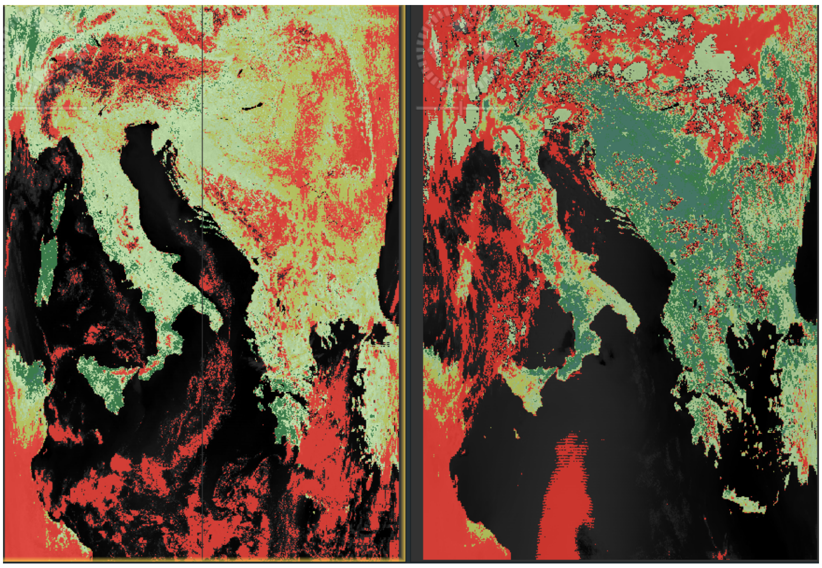

Figure 19: On the left the the winter NDVI, on the right summer

6.5 Change Detection

Change detection is a process that measures how the attributes of a particular area have changed between two or more time periods. In our case the change is referred to the NDVI difference over the two seasons. In order to do that it is necessary to reproject the products over the same grids and using *Band Maths* tool applying a difference between NDVI on winter and summer. Results are visible in fig. **??**. It is possible to see areas where this difference is very high, maybe because there are pruned crop fields, or due to the lack of irrigation in the zone.

References

[1] R. B. Myneni, F. G. Hall, P. J. Sellers, and A. L. Marshak. The interpretation of spectral vegetation indexes. *IEEE Transactions on Geoscience and Remote Sensing*, 33(2):481–486, 1995.

[2] A. Viña, A. A. Gitelson, A. L. Nguy-Robertson, and Y. Peng. Comparison of different vegetation indices for the remote assessment of green leaf area index of crops. *Remote Sensing of Environment*, 115(12):3468–3478, 2011.